

1 **Mutation-induced infections of phage-plasmids**

2 Xiaoyu Shan¹, Rachel E. Szabo^{1,2}, Otto X. Cordero^{1*}

3 1. Department of Civil and Environmental Engineering, Massachusetts Institute of Technology

4 2. Microbiology Graduate Program, Massachusetts Institute of Technology

5 *Corresponding author. Email: ottox@mit.edu

6 **Abstract**

7 Phage-plasmids are extra-chromosomal elements that act both as plasmids and as phages, whose
8 eco-evolutionary dynamics remain poorly constrained. Here, we show segregational drift and loss-
9 of-function mutations play key roles in the infection dynamics of a cosmopolitan phage-plasmid,
10 allowing it to create continuous productive infections in a population of marine *Roseobacter*.
11 Recurrent loss-of-function mutations in the phage repressor that controls prophage induction led to
12 constitutively lytic phage-plasmids that spread rapidly throughout the population. The entire phage-
13 plasmid genome was packaged into virions, which were horizontally transferred by re-infecting
14 lysogenized cells, leading to an increase in phage-plasmid copy number and to a heterozygous phage
15 repressor locus within re-infected cells. While wild-type repressor variants prevented induction of
16 phage-plasmids in a cell, the uneven apportionment of phage-plasmids after cell division (i.e.,
17 segregational drift) led to the production of offspring carrying only the constitutively lytic phage-
18 plasmid, thus restarting the lysis-reinfection-segregation life-cycle. Mathematical models and
19 experiments showed that these dynamics lead to a continuous productive infection of the bacterial
20 population in which lytic and lysogenic phage-plasmids coexist. An analysis of marine bacterial
21 genomes shows that the same plasmid backbone here described carries different phages in the
22 environment and disseminates trans-continentially, suggesting that the phage-plasmid strategy is
23 relevant and widespread in nature. Together, our study describes how the interplay between phage
24 infection and plasmid genetics provide a unique eco-evolutionary strategy for phage-plasmids.

26 **Introduction**

27 A key distinction among temperate phages is whether they integrate into the host chromosome (e.g.,
28 the well-known *Escherichia coli*'s phage lambda) or replicate as an extrachromosomal element. In
29 this latter group are phage-plasmids, circular elements that appear to have evolved by the fusion of
30 a plasmid and phage. Although a few examples such as *Escherichia coli* P1¹ infecting *Escherichia*
31 *coli* and *Vibrio cholerae* VP882² have been extensively-studied, it is only very recently we that we
32 have become aware of the prevalence and relevance of these hybrid elements³. Recent surveys have
33 found that phage-plasmids are abundant^{3,4} and carry a large diversity of clinically relevant antibiotic
34 resistant genes across bacteria⁵. Despite their significance, however, most of these elements have
35 not been experimentally characterized and their ecology and evolution as not only phages but also
36 plasmids remain poorly understood.

37 As most other plasmids, phage-plasmids can also be found in multiple copies per cell
38 (polyploidy). This fact has surprising implications for the population genetics of these elements and
39 their dynamics of infection. Polyploidy makes it possible for cells to be heterozygous at any phage-
40 plasmid encoded locus⁶⁻⁸, including key genes such as the transcriptional repressor that maintains
41 the phage in its lysogenic state. This intra-cell genetic variation can have a significant impact on
42 phage-plasmid dynamics. If the prophage was chromosomally integrated, loss of function mutations

44 in the phage repressor would be effectively suicide mutations, committing the phage to a lytic phage.
45 However, in theory, such defective allele variants could be recessive in a polyploid phage-plasmid.
46 Polyploidy also implies that the intergenerational dynamics of phage-plasmids are affected by
47 segregational drift – i.e., the random assortment of plasmid copies among daughter cells after cell
48 division. Segregational drift can lead to large fluctuations in the degree of heterozygosity (including
49 the production of homozygous offspring) in subsequent generations^{9–11}. As shown below, the
50 interplay between heterozygosity and segregational drift in phage-plasmids can lead to a type of
51 eco-evolutionary dynamics unique for phage-plasmids.

52 We explore these dynamics focusing on a cosmopolitan type of phage-plasmid widespread
53 among marine *Roseobacter* – an abundant copiotroph in the ocean¹². Using a combination of
54 experiments and mathematical models we show that the hybrid nature of phage-plasmids allows
55 loss-of-function mutations in the phage repressor gene to be maintained in the population, leading
56 to continuous productive infections. We show that phage-plasmid variants transmit rapidly
57 throughout the population via horizontal transfer, increasing ploidy and producing heterozygous
58 cells. This force is counterbalanced by segregational drift, which restores homozygosity. The
59 combination of these forces leads to the continuous production of phages and the stable coexistence
60 of infected and resistance cells. We continue to show that the phage-plasmids such as this are formed
61 frequently in the environment via fusion of plasmid backbones and phages and widespread across
62 disparate geographic regions, suggesting a successful life-style strategy for these parasitic elements.
63

64 Results

65 Recurrent productive infection of a phage-plasmid in *T. mobilis* after ~40 generations

66 *Tritonibacter mobilis* (previously known as *Ruegeria mobilis*) is a member of the *Roseobacter*
67 clade¹², which collectively represents one of the most ubiquitous groups of marine heterotrophic
68 bacteria¹³. *Tritonibacter mobilis* A3R06, carrying a temperate phage-plasmid, was isolated from an
69 agarose particle inoculated with coastal seawater bacterial communities. Its genome has 4.65 million
70 base pairs (Mbp), with a chromosome of 3.2 Mbp plus four (mega)plasmids of 1.2 Mbp, 0.1 Mbp,
71 78 thousand base pairs (Kbp) and 42 (Kbp), respectively (Figure S1). The 42 Kbp plasmid is also a
72 circular phage with 51 predicted genes. These include genes encoding a phage head, tail, capsid and
73 portal proteins, lysozyme, cell wall hydrolases as well as a C1-type phage repressor. The rest of the
74 genes are involved in plasmid stability, replication and segregation, such as the *yoEB-yeM* toxin-
75 antitoxin system, the *parAB* plasmid segregation system and P4-family plasmid primase (Figure S2).

76 We observed productive infection of the phage-plasmid after ~40 generations (Figure 1A)
77 when *Tritonibacter mobilis* A3R06 was grown under serial dilution cycles of approximately 6
78 generations (~ 24 hours) in minimal media (Figure S3). Remarkably, we found that productive
79 infection happened in all of 15 independent biological replicates after 30~50 generations (Figure
80 1A, Table S1 and Figure S4). Productive infection of the phage-plasmid resulted in a sharp decline
81 in optical density (OD600) in all the populations (Figure 1a and Figure S4), due to the formation of
82 cell clumps (Figure S5). Fluorescence staining indicated the presence of extracellular DNA (eDNA)
83 inside clumps (Figure S5), consistent with the idea that cell lysis promoted clump formation¹⁴. To
84 validate the lysogeny-lysis switch of the phage-plasmid, we did transmission electron microscopic
85 imaging for the 0.22 μ m filtered supernatant of the clumpy bacterial culture, confirming the
86 production of virion particles. The phage particle has *Siphoviride*-type morphology, with an

87 isometric head of ~ 50 nm diameter and a long tail of ~ 180 nm length (Figure 1B).

88

89 **Productive infection of the phage-plasmid is driven by mutations in a phage repressor region**

90 The observed 30-50 generation lag before the productive infection suggested that the lysogenic-lytic
91 switch was less likely to be driven by metabolite accumulation or physiological signaling.
92 Alternatively, we hypothesized that the prophage induction was driven by genotypic changes. To
93 test this hypothesis, we did genomic sequencing for 9 independent bacterial populations at the end
94 of each dilution cycle. We found that only a short, ~1000 bp region in the phage genome encoding
95 a C1-type phage repressor, consistently contained mutations across all the independent lines (Figure
96 1D, Table S1). A large fraction (15/19, 78.9%) of the mutations were insertion/deletion mutations
97 leading to frame-shift within either the helix-turn-helix DNA binding domain of the C1-type
98 repressor or the putative upstream promoter region as inferred from the level of transcripts (Figure
99 1D), suggesting that the mutations resulted in a loss of repressor function. Interestingly, a majority
100 of these insertion/deletion mutations (9/15, 60.0%) were related to tandem repeats sequences in the
101 genome (e.g., nucleotide position 11897: from GAAAAA to GAAAA, Table S1), which act as
102 mutational hotspots due to replication slippage¹⁵⁻¹⁷, suggesting that these mutations occurred faster
103 than the background rate.

104 In order to learn more about the consequences of the repressor mutations, we performed RNA-
105 seq experiments for 3 independent populations, which allowed us to quantify the transcription of
106 phage coding sequences before and after the mutation was observed. We found that the expression
107 of genes related to a lytic phage lifestyle in the phage-plasmid were highly up-regulated after the
108 observation of mutations in the repressor sequence, such as the phage capsid, phage tail and
109 lysozyme (128~256 folds, Figure 1C), showing these genes related to phage production were indeed
110 de-repressed after the loss-of-function mutations. In contrast, those genes related to plasmid
111 replication and stability such as the *yoEB-yefM* toxin-antitoxin system and the *parAB* plasmid
112 segregation system were only increased similarly with the copy-number increase of the phage-
113 plasmid (2~4 folds, Figure 1C). These genes were actively expressed even before the mutation was
114 observed (Figure S6), suggesting that they were functioning for a lysogenic lifestyle.

115 DNA sequencing across different timepoints during dilution cycles showed that, after repressor
116 mutations appeared, their frequency in the population increased at an extremely rapid rate. e.g.,
117 jumping to ~50% within one dilution cycle of 6 generations in a population of ~10⁸ cells. Despite
118 this rapid increase, the mutant genotype never reached fixation, stabilizing at around 60% (Figure
119 1A and Figure S4). This pattern of evolutionary dynamics was intriguing in two respects. First, if
120 transmission was only vertical, the drastic increase in the mutant genotype frequency would imply
121 unrealistically high relative fitness coefficients (s ~ 100). Therefore, the evolutionary dynamics can
122 only be explained by the infection spreading horizontally throughout the population. This presents
123 an apparent conundrum, as we expected a host population lysogenized with the wild-type phage-
124 plasmid to be immune to the same type of phage^{18,19}. Second, if the mutated phage genotype was
125 able to spread so rapidly throughout the population, why did not it reach fixation?

126

127 **Reinfection and segregational drift together explain the observed evolutionary dynamics**

128 We hypothesized that the observed evolutionary dynamics could be explained by the unique
129 population genetic features of a phage-plasmid hybrid. If the mutated phage was able to spread

130 through the population via virion production and reinfection, then the infected cells would likely
131 contain multiple plasmid copies and be heterozygous at the repressor locus (e.g., one copy of
132 lysogenic wild-type phage plasmid and one copy of mutated phage plasmid). In that case,
133 segregational drift during the stochastic partitioning of plasmids between daughter cells should
134 impact the subsequent bacterial and phage population dynamics. Indeed, recent studies have shown
135 that the evolution of multiple-copy plasmids is affected by segregational drift^{6,9,10}, akin to the case
136 of mitochondria in eukaryotes¹¹, resulting in variation in intracellular frequencies of plasmid-
137 encoded alleles between mother cells and daughter cells. In the simplest scenario where plasmids
138 were randomly distributed into daughter cells with equal opportunity, while the copy number of
139 plasmids per cell remained constant, cell division could result in the maintenance of repressor
140 heterozygosity at the single cell level, or the production of two homozygote cells, one carrying only
141 wild-type and one carrying only mutated phage (Figure S7). In the latter case, the daughter cell with
142 only mutated phages would be lysed, releasing more mutated phage particles and continuing the
143 spread of the phage.

144 Further experiments confirmed that the lytic phage-plasmid re-infected cells lysogenized with
145 wild-type (Figure 2A-B). To show this, we spiked cell-free supernatant containing the mutant phage-
146 plasmid into a culture of the host carrying only the wild-type variant. After an overnight incubation
147 we observed the appearance of clumps, identical to those that appear spontaneously after 30-50
148 generations (Methods). Genome sequencing of clones streaked out of this culture showed that they
149 carried the full mutant phage-plasmid, whose genotype were identical to the one of present in the
150 cell-free supernatant used in the re-infection experiment, and that they were heterozygous at the
151 repressor locus (Figure 2B). In contrast, when we repeated the same experiment but with the cell-
152 free supernatant 0.02 μ m filtered to remove the phage particles, the victim host population remained
153 planktonic, indicating no re-infection.

154 As a result of re-infection, we observed an increase in phage-plasmid copy number, opening
155 the possibility for segregational drift to impact its evolutionary dynamics (Figure 2C-D). Starting
156 with a single colony carrying both the wild-type and mutant phage-plasmids, we questioned whether
157 it was able to generate homozygous descendants, carrying only wild-type phages (Methods). As
158 expected, we found that a heterozygous mother host cell was able to produce offspring that are free
159 of the mutant phage. Genome sequencing of four post-segregation descendant populations
160 confirmed that they only contained the wild-type phage-plasmid and its average copy number was
161 significantly increased (Figure S8, Kruskal-Wallis test $P = 0.02$) as a consequence of segregational
162 drift (Figure 2C).

163 A higher dosage of wild-type repressor gene copies should in principle provide a stronger
164 buffer against phage-plasmid induction, at least in part because the probability of generating zero
165 wild-type repressor after segregational drift would be lower. To test this, we restarted the serial
166 dilution cycles with the post-segregation populations carrying a higher copy number of wild-type
167 phages. Indeed, we found that it took at least 66 generations to observe phage-plasmid induction
168 (Figure S9), which was significantly longer than the 30~50 generations observed for wild-type
169 populations with single-copy repressor gene.

170 With reinfection and segregational drift as the only two basic components, we found that a
171 minimal probabilistic model was sufficient to reproduce the observed evolutionary dynamics of the
172 phage-plasmid mutations (Figure 3 and Methods for full details of simulation). We started with a

173 population of one million host cells each carrying a single copy of wild-type phage-plasmid and
174 doubling 6 times per serial passage exactly the same as in the experimental condition (Method). A
175 loss-of-mutation happened in a random phage-plasmid, leading to the lysis of host cell and release
176 of mutated phage-plasmid particles. Some of the released phage-plasmids managed to reinfect
177 another randomly-encountered host based on an efficiency of re-infection (R), which is reminiscent
178 of the production efficiency (R_0) in epidemiology (Methods). The re-infected hosts carrying only
179 heterozygous repressor loci underwent segregational drift, after which descendants carrying only
180 mutated phage-plasmids were lysed and re-entered the infection cycle. With these ingredients, our
181 simulation displayed a rapid spread of the mutated phage infection before quickly saturating, which
182 is consistent with experimental observations (Figure 3).

183

184 **Dissemination of phage-plasmids across geographic and phylogenetic distances**

185 Using comparative genomics, we found that the plasmid backbone of the *Tritonibacter mobilis*
186 A3R06 phage-plasmid carries different phage head and tail components across different continents
187 (Figure 4). To better understand the ecological distribution of phage-plasmids, we leveraged 1,849
188 genomes available in the RefSeq database from the order of *Rhodobacterales*, to which the
189 *Tritonibacter mobilis* was affiliated. With these genomes, we searched for homologs of the phage-
190 related genes or plasmid-related genes in our *Tritonibacter mobilis* phage-plasmid (isolated in
191 Massachusetts, USA). Strikingly, we found clusters of nearly identical (~ 100%) homologs of
192 plasmid-related genes, such as *parAB* segregation system and P4-family plasmid primase, in another
193 phage-plasmid of another *Tritonibacter mobilis* strain isolated in marine aquaculture in Denmark¹²
194 (Figure 4). These gene clusters were also found in perfect synteny, which strongly indicated a
195 recombination event. However, the phage structural genes (e.g., phage head and tail) of these two
196 phages were very different, both in terms of homology and synteny. The structural genes of our
197 *Tritonibacter mobilis* phage-plasmid was both homologous and syntenic to those found in another
198 phage integrated in the genome of a *Roseobacter* strain, which was isolated from 2,500 m deep
199 water in the Arabian Sea²⁰ (Figure 4). Taking together, our results showed that the evolution of the
200 plasmid-related genes and the phage-related genes for phage-plasmids could be decoupled. Different
201 phages could become the genetic cargo of the same plasmid, which was able to transmit across
202 continents carrying their phage components. This was consistent with recent findings showing that
203 the core plasmid backbone could be recombined with different cargo genes in marine or human gut
204 microbiome^{21,22}, with our findings suggesting that this could be exploited by phages to disseminate
205 across large geographic distances. Additionally, we identified a second example of nearly identical
206 plasmid-related genes but very different phage-related genes between two other phage-plasmids^{23,24}
207 (Figure S11). These two phages were found in two strains of different though related bacterial
208 species (average nucleotide identity ~92%), suggesting that plasmid backbones were also able to
209 transmit across phylogenetic distances. All those phage-plasmids resemble *Tritonibacter mobilis*
210 A3R06's phage-plasmid: a 4K-5K genome size with the presence of independent replication systems
211 (such as *ParABS* and *RepABC*) but absence of genes known for effective reinfection blockage (such
212 as *SieA* of *E.coli* phage P1¹⁹), suggesting those phages can be also subject to mutation-driven
213 induction in natural environment.

214 A bioinformatic search across publicly available metagenomes identified significant hits ($e <$
215 10^{-15}) of the *Tritonibacter mobilis* A3R06 phage-plasmid repressor in several natural microbial

216 communities across the globe (Figure S12). Hits were found mainly in nutrient rich marine
217 environment, such as an shrimp aquaculture in the eastern coast of China²⁵, particle-attached
218 Mediterranean water column²⁶, as well as an intense algal bloom in California²⁷. Further studies are
219 required to get more complete sequence information of phage-plasmids and to capture and
220 characterize their eco-evolutionary dynamics in natural environments.

221

222 Discussion

223 In this study, we found that mutation and segregational drift controlled the dynamics of transmission
224 of a cosmopolitan phage-plasmid. First, we showed that a spontaneously mutated phage-plasmid
225 was able to re-infect a host lysogenized with a wild-type phage, which prevented the mutant phage-
226 plasmid from turning lytic. Second, we showed that segregational drift diversified the phenotypic
227 outcomes of daughter cells, with cells carrying only mutant phage-plasmids lysing and releasing
228 virions. These observations reflect a mixture of both phage and plasmid properties – the phage facet
229 enables rapid horizontal proliferation through virion production while the plasmid facet enables
230 heterozygosity and segregational drift. Consequently, the phage-plasmids proliferated rapidly
231 through iterative reinfection and lysis of a stochastically selected proportion of host descendants,
232 leading to the co-existence of mutant phages and wild-type phage-plasmids. This strategy also
233 reflects how genes and alleles can use viruses to rapidly propagate through a population without
234 driving it to a sudden collapse.

235 The mutation-driven switch from lysogeny to lysis we observed in this study is distinct from
236 the traditional model of prophage induction as a regulatory response to stress, chemical signaling,
237 etc. The rate of mutation-driven induction should be proportional to the rate of mutation
238 accumulation in a population. Therefore, rapidly growing host population with large population
239 sizes can develop continuous productive infections, as observed in this study. This might be
240 ecologically relevant considering the “opportunitrophic” lifestyle of *Roseobacter* in the marine
241 environment²⁸. Members of this clade are well known to routinely switch between two types of
242 ecological scenarios, i.e., maintenance of survival with low abundance in the bulk oligotrophic
243 ocean, and rapid growth on transient nutritional hotspots such as the phycosphere of marine algae²⁹.
244 Mutation-driven prophage induction is more likely to happen in the latter situation where bacterial
245 hosts grow rapidly and reach high local densities, allowing transmission by virion reinfection.
246 Therefore, the ecology of this plasmid-phage and its host are likely intimately related.

247 We found that the phage plasmids such the one here described evolve by the rapid mixing and
248 matching of plasmid backbones and prophages. This is evident in the fact that the phage region of
249 the phage-plasmid was homologous to a phage found in the Arabian Sea, while its plasmid backbone
250 was homologous to another phage-plasmid found in Denmark. Considering that the element that is
251 the focus of this paper was isolated from the coast of Massachusetts, we conclude that phage
252 plasmids are evolutionary chimeras that combine elements with disparate evolutionary histories and
253 disseminate across vast geographic distances. The wide distribution of these elements in natural
254 environment and their ability to maintain continuous productive infections with rapid transmission
255 of new genetic variants, suggest that these elements may be major vectors of horizontal transfer.
256 Further work is needed to better-understand the ecological relevance of this hybrid elements and
257 their potential of mutation-driven induction to trigger continuous productive infections in natural
258 and synthetic systems.

259

260 Methods

261 Media

262 The minimal marine media, MBL media, was used for serial dilution growth of *Tritonibacter mobilis*
263 A3R06. It contained 10 mM NH₄Cl, 10 mM Na₂HPO₄, 1 mM Na₂SO₄, 50 mM HEPES buffer (pH
264 8.2), NaCl (20 g/liter), MgCl₂*6H₂O (3 g/liter), CaCl₂*2H₂O (0.15 g/liter), and KCl (0.5 g/liter).
265 Glucose was added as the only carbon source at a concentration of 27 mM. Trace metals and
266 vitamins were added by 1:1000 of the following stock solution. Trace metals stock solution included
267 FeSO₄*7H₂O (2100 mg/liter), H₃BO₃ (30 mg/liter), MnCl₂*4H₂O (100 mg/liter), CoCl₂*6H₂O (190
268 mg/liter), NiCl₂*6H₂O (24 mg/liter), CuCl₂*2H₂O (2 mg/liter), ZnSO₄*7H₂O (144 mg/liter),
269 Na₂MoO₄*2H₂O (36 mg/liter), NaVO₃ (25 mg/liter), NaWO₄*2H₂O (25 mg/liter), and
270 Na₂SeO₃*5H₂O (6 mg/liter). Vitamins, which were dissolved in 10 mM MOPS (pH 7.2), contained
271 riboflavin (100 mg/liter), D-biotin (30 mg/liter), thiamine hydrochloride (100 mg/liter), L-ascorbic
272 acid (100 mg/liter), Ca-D-pantothenate (100 mg/liter), folate (100 mg/liter), nicotinate (100
273 mg/liter), 4-aminobenzoic acid (100 mg/liter), pyridoxine HCl (100 mg/liter), lipoic acid (100
274 mg/liter), NAD (100 mg/liter), thiamine pyrophosphate (100 mg/liter), and cyanocobalamin (10
275 mg/liter). Marine Broth 2216, a rich media commonly used for growing marine bacterial strains,
276 was purchased from the Fisher Scientific (BD 279110).

277 Culture growth

278 Single colonies of *Tritonibacter mobilis* A3R06 on Marine Broth agar plates were picked for
279 enrichment in 2 mL liquid Marine Broth 2216 media for 6 hours. After that, 50 µL of enriched
280 culture was transferred into 4 mL MBL minimal media for pre-culture growth. Cells in the pre-
281 culture was grown to mid-exponential phase before being diluted into 4 mL fresh MBL minimal
282 media to an OD600 of roughly 0.01 to initiate the serial dilution cycles. Each cycle lasted for 24
283 hours, corresponding to roughly 6 generations per cycle considering the doubling time of
284 *Tritonibacter mobilis* A3R06 being ~ 4 hours in MBL minimal media with glucose (Figure S3). At
285 the end of each cycle, cells were still within the exponential phase of growth (Figure S3), except for
286 those very late cycles where cell clump formed following the productive switch of the phage-
287 plasmid. All liquid culture growth was performed in Innova 42R incubator shaking at 220 rpm at
288 25°C.

289 DNA extraction, Illumina sequencing and reads processing

290 Prior to DNA extraction, the cell culture samples were centrifuged at 8000 g for 60 seconds to
291 remove the liquid. The cells were then resuspended into fresh MBL media by thoroughly pipetting
292 for at least fifteen times. For each sample, the resuspension-centrifuge procedure was repeated for
293 three times so as to wash away free virion particles outside of the cells. For Illumina sequencing,
294 DNA was extracted with the Agencourt DNAAdvance Genomic DNA Isolation Kit (Beckman
295 Coulter). DNA concentration was quantified with Quant-iT PicoGreen dsDNA Assay kit (Invitrogen)
296 on a Tecan plate reader. Short-read sequencing was performed on an Illumina NextSeq 2000
297 platform (2x151bp pair-ended). Library preparations and sequencing were performed at the
298 Microbial Genome Sequencing Center (Pittsburgh, PA). Sequencing reads were trimmed to remove
299 adaptors and low-quality bases (-m pe -q 20) with Skewer v0.2.2³⁰. The remaining paired reads were
300 checked for quality with FastQC v0.11.9.

301 Closing the genome of *Tritonibacter mobilis* A3R06

302 Nanopore long-read sequencing was used to close the genome of *Tritonibacter mobilis* A3R06. DNA
303 was extracted with a Qiagen DNeasy kit for higher DNA yield following the manufacturer's protocol.
304 Long-read sequencing was performed on the Oxford Nanopore platform with a PCR-free ligation
305 library preparation at the Microbial Genome Sequencing Center (Pittsburgh, PA). Closed genome
306 of *Tritonibacter mobilis* A3R06 was assembled using Unicycler v0.4.9³¹ by combining Illumina
307 short reads and Nanopore long reads, resulting in one chromosome plus four circular plasmids. The
308 assembly graph in gfa format was visualized by Bandage v0.8.1³². Coding sequences were predicted
309 using prodigal v2.6.3³³ and functionally annotated with eggNOG-mapper v2³⁴ (--go_evidence non-
310 electronic --target_orthologs all --seed_ortholog_evalue 0.001 --seed_ortholog_score 60). The
311 phage genome map was visualized by SnapGene v6.0 (Insightful Science; available at
312 snapgene.com).

313 **Read mapping and variant calling**

314 The complete genome of *Tritonibacter mobilis* A3R06 was used as the reference genome. Quality-
315 filtered pair-ended Illumina sequencing reads were mapped the reference genome using Minimap2
316 v2.17 with stringent settings (-ax sr)³⁵. Genetic variants were identified from the aligned reads using
317 BCFtools with only variants with quality score ≥ 20 and a local read depth ≥ 20 were remained³⁶.

318 **RNA isolation and sequencing**

319 RNA Protect Bacterial Reagent (Qiagen, Hilden, Germany) was added to the cell culture samples
320 at a 2:1 volume ratio. RNA was isolated with a Qiagen RNeasy kit following the manufacturer's
321 protocol except for the following changes³⁷: cells were resuspended in 15 mg/mL lysozyme in TE
322 buffer and incubated for 30 min at room temperature before adding buffer RLT. Mechanical
323 disruption of samples using lysing matrix B (MPBio, Santa Ana, CA) were performed by shaking
324 in a homogenizer (MPBio) for 10X 30 seconds intervals. Dry ice was added in the homogenizer to
325 prevent overheating. Illumina Stranded RNA library preparation with RiboZero Plus rRNA
326 depletion and pair-ended Illumina sequencing (2x51bp) were performed at the Microbial Genome
327 Sequencing Center (Pittsburgh, PA).

328 **Transcriptomic analysis**

329 Paired-end RNA reads were trimmed using Skewer v0.2.2 to remove sequencing adapters and low-
330 quality reads (-m pe -q 20)³⁰. The remaining paired reads were checked for quality with FastQC
331 v0.11.9 and mapped to *Tritonibacter mobilis* A3R06 genome using Bowtie2 v2.2.6³⁸. The generated
332 SAM files were sorted by position using SAMTools v1.3.1³⁶. Count table of transcripts were
333 obtained by HTSeq v0.11.3³⁹ and differential gene expression was evaluated with DeSeq2 R
334 package⁴⁰. Normalized transcript abundance was generated from count tables by transcripts per
335 kilobase million (TPM) calculations.

336 **Fluorescence staining and light microscope**

337 Live cells were stained by 5 μ M SYTO9 which emits green fluorescence when it is bound to DNA.
338 Dead cells were stained by 20 μ M propidium iodide which emits red fluorescence when it is bound
339 to DNA but was unable to permeate the cell membrane. Fluorescence was visualized using an
340 ImageXpress high content microscope equipped with Metamorph Software (Molecular devices, San
341 Jose, CA), operating in widefield mode. Images were acquired in widefield mode at 40x with a Ph2
342 ELWD objective (0.6 NA, Nikon) and filter sets: Ex 482/35 nm, Em: 536/40 nm, dichroic 506 nm
343 to detect SYTO9 and Ex 562/40 nm, Em 624/40 nm, dichroic 593 nm to detect propidium iodide.
344 Images were collected with exposure times of 100 ms and processed with ImageJ v1.53⁴¹.

345 **Transmission electron microscopic imaging**

346 Transmission electron microscopic imaging was performed at Koch Institute's Robert A. Swanson
347 (1969) Biotechnology Center Nanotechnology Materials Core (Cambridge, MA). Samples were
348 negatively stained with 2% uranyl acetate and were imaged on an JEOL 2100 FEG microscope. The
349 microscope was operated at 200 kV and with a magnification in the ranges of 10,000~60,000 for
350 assessing particle size and distribution. All images were recorded on a Gatan 2kx2k UltraScan CCD
351 camera.

352 **Comparative genomics of Rhodobacterales phages**

353 A total of 1,849 genomes in the Family of *Rhodobacterales* were downloaded from NCBI RefSeq
354 database on Jan 1st 2022. Coding sequences were annotated by eggNOG-mapper v2 (--go_evidence
355 non-electronic --target_orthologs all --seed_ortholog_eval 0.001 --seed_ortholog_score 60)³⁴.
356 Phage sequences were predicted with VIBRANT v.1.2.0⁴². MMseqs2⁴³ was used to search for search
357 for homologs of *Tritonibacter mobilis* A3R06 phage genes, with high sensitivity parameters (-s 7.5
358 -c 0.8). The search output of MMseqs2 were sorted for the most significant hits as well as the highest
359 number of hits, leading to the finding of *Tritonibacter mobilis* M41-2.2 phage and *Roseobacter* sp.
360 SK209-2-6 phage.

361 **Model simulation of eco-evolutionary dynamics**

362 In order to simulate the evolutionary dynamics of the phage-plasmid, we developed a minimal
363 model combining the population genetics of a plasmid as well as infection dynamics of a phage.
364 Our model in part resembles a classical Wright-Fisher model, which assumes non-overlapping
365 generations in a discrete Markov process. However, we considered dynamic population size in our
366 model, which incorporates cell doubling within a serial dilution cycle as well as cell lysis due to
367 phage production. To start with, we have a population of N_0 host cells. When there is no phage-
368 plasmid productive infection, all cells divide into two daughter cells thus the population size doubled
369 every generation following $N_t = N_0 2^t$, which reaches $2^6 \times N$ at the end of each serial dilution
370 cycle. Then a bottleneck indicated by the dilution factor d was applied to the population so that
371 $1/d$ cells were randomly sampled from the current population to enter the next serial dilution cycle.
372 In our simulation, we use $N = 10^6$ at the beginning of each dilution cycle and dilution factor $d =$
373 64 as we did in experiment. Each host cell carries one copy of wild-type lysogenic phage-plasmid,
374 replicating and segregating into two daughter cells as the host cell divides.

375 When a loss-of-function mutation happens in one of the phage-plasmids, the lysogenic phage
376 switches to be lytic due to silence of the phage repressor. The host cell carrying the mutated phage-
377 plasmid is then killed, releasing virion particles with the mutated phage genome to randomly infect
378 other host cells. Previous studies have reported burst size of marine prokaryotic phages ranging
379 from 4 to more than 100⁴⁴. In our model, what matters in population genetics is the average number
380 of released mutated phage-plasmids that successfully re-infect a host cell per host cell lysed. This
381 parameter, termed as re-infection efficiency R , is similar to the parameter R_0 in epidemiology and
382 should be lower than the empirical burst sizes⁴⁵, especially considering that the other host cells have
383 been already lysogenized with a wild-type phage-plasmid larger than 40KB. We found that the
384 saturating frequency of the mutated genotype was affected by R , for which $R = 5$ best fitted the
385 experimentally observation (Figure S10).

386 The host cells re-infected by the mutated phage-plasmids become heterozygote with more than one
387 copies of phage-plasmids. Segregation of multiple copies of phage-plasmids with different

388 genotypes can lead to genetic heterogeneity among daughter cells. In our minimal model, we assume
389 a simplest scenario where phage-plasmids were randomly distributed into daughter cells with equal
390 opportunity, while the copy number of plasmids per cell remained constant. For a cell host with a
391 copies of wild-type phage-plasmids and b copies of mutated phage-plasmids, the segregation can
392 be described using a Binomial distribution $B(2a + 2b, a + b)$. For instance, the probability of
393 having a_1 copies of wild-type phage-plasmids in the first daughter cell follows

$$P(a_1) = C_{2a}^{a_1} C_{2b}^{a+b-a_1} / C_{2a+2b}^{a+b}$$

394 To simulate segregational drift at cell division, we performed Binomial sampling for all
395 heterozygotic cell hosts containing more than one copies of phage-plasmids at each generation,
396 generating daughter cells with stochastically different genotypes. Cells carrying at least one copy of
397 wild-type phage-plasmid are prevented from lysis since the repressor gene is normally functioning.
398 Host cells carrying only mutated phage-plasmids after segregational drift will be killed since the
399 lytic genes on the phage-plasmids are no longer repressed. These lysed cells will be used to produce
400 more virion particles to re-infect more host cells in the next cycle.
401

402 **Experimental confirmation of reinfection**

403 To verify re-infection, mutated phage-plasmids were used to infect the host population carrying the
404 wild-type phage-plasmid. Mutated phage-plasmids were separated from the source host population
405 cells by filtering through a 0.22 μm pore size membrane. The supernatant was then spiked into a
406 victim host population carrying only wild-type phage-plasmids growing in fresh MBL minimal
407 media. The planktonic culture became highly clumpy after overnight growth, indicative of phage-
408 plasmid induction. The infected population was then used to streak an agar plate for descendant
409 single colonies. Colonies considered to harbor the mutated phage through re-infection, as indicated
410 by the clump formation after re-growing in liquid media, were sequenced for phage-plasmid
411 genotyping. The experiment was performed in biological duplicates with two source host
412 populations carrying different mutated genotypes (11366: A→AT and 11853: C→T).

413 **Experimental confirmation of segregational drift**

414 To verify segregational drift, host populations carrying both wild-type phages and mutated phages
415 were tested for whether they were able to generate offspring with only wild-type phages. To ensure
416 the host population really came from a heterozygote single cell rather than a clump of cells with
417 mixed genotypes, we filtered the host population carrying mutated phages with 1 μm cell strainer
418 (Pluriselect 437000103) to remove the multicellular clumpy aggregates. The filtered planktonic
419 subpopulation was carefully examined under the microscope to ensure it contained planktonic cells
420 clearly separated from each other. We then streaked this planktonic subpopulation on an agar plate
421 for single colonies, of which 4 single colonies carrying both wild-type and mutated phages were
422 picked as mother colonies. For each mother colony, liquid culture after overnight growth was then
423 used to streak agar plates for daughter colonies, of which 12 daughter colonies were picked per
424 mother colony. All the 48 daughter colonies were screened in liquid culture for whether they were
425 planktonic, which is indicative of carrying only wild-type phage-plasmids, or clumpy, which is
426 indicative of induction of mutated phage-plasmids. Further, we performed whole-genome
427 sequencing of four daughter colonies that are planktonic in liquid culture, confirming that 1) they
428 were indeed free of any mutated phage-plasmids and only contained wild-type phage-plasmids and
429 2) the copy number of phage-plasmid in their genomes are significantly increased.

430 **Phage susceptibility of other Rhodobacterales strains**

431 The *yoeB-yefM* toxin-antitoxin system encoded by the phage-plasmid makes it difficult to cure the
432 plasmid for the *Tritonibacter mobilis* A3R06 host. We therefore tried to test whether this phage-
433 plasmid is able to infect any other bacterial host with a plaque assay, including *Tritonibacter mobilis*
434 F1926 which is the model strain for the *Tritonibacter* genus¹² and other 28 *Rhodobacterales* isolates
435 in the Cordero lab strain collection. However, none of those isolates were subject to infection.
436 Recent studies suggested that specificity of phage infection may be related to the structure of
437 bacterial capsule. This may be the case for our phage-plasmid since *Tritonibacter mobilis* A3R06
438 harbors another 78Kb plasmid encoding a capsule, which was not found in the genome of other
439 strains we tested for susceptibility.

440

441 **Acknowledgement**

442 We thank Professors Lone Gram, Tami Lieberman and Terence Hwa for their help and suggestions
443 to this work. We thank Gabriel Vercelli, Jie Yun, Fatima Hussain, Sammy Pontrelli and all Cordero
444 lab members for helpful discussions. We thank MIT Koch Institute's Robert A. Swanson (1969)
445 Biotechnology Center for technical support, in particular Dr. Dongsoo Yun with the JEOL 2100 FEG
446 microscope (RRID:SCR_018674). O.X.C and X.S were supported by the Simons Collaboration:
447 Principles of Microbial Ecosystems, award number 542395.

448

449 **Data accession**

450 Closed genome of *Tritonibacter mobilis* A3R06 is available at NCBI under accession number
451 PRJNA895449. Genomic and transcriptomic sequences for experimental evolution lines are
452 available at NCBI under accession number SAMN31509900. All data is to be released to public
453 upon publication.

454

455 **Reference**

- 456 1. Hoess, R. H., Ziese, M. & Sternberg, N. P1 site-specific recombination: nucleotide sequence of
457 the recombining sites. *Proc. Natl. Acad. Sci. U. S. A.* **79**, 3398 (1982).
- 458 2. Silpe, J. E. & Bassler, B. L. A Host-Produced Quorum-Sensing Autoinducer Controls a Phage
459 Lysis-Lysogeny Decision. *Cell* **176**, 268-280.e13 (2019).
- 460 3. Gilcrease, E. B. & Casjens, S. R. The genome sequence of *Escherichia coli* tailed phage D6 and
461 the diversity of *Enterobacteriales* circular plasmid prophages. *Virology* **515**, 203–214 (2018).
- 462 4. Pfeifer, E., Moura De Sousa, J. A., Touchon, M. & Rocha, E. P. C. Bacteria have numerous
463 distinctive groups of phage-plasmids with conserved phage and variable plasmid gene
464 repertoires. *Nucleic Acids Res.* **49**, 2655–2673 (2021).
- 465 5. Pfeifer, E., Bonnin, R. A. & Rocha, E. P. C. Phage-plasmids spread antibiotic resistance genes
466 through infection and lysogenic conversion. *bioRxiv* 2022.06.24.497495 (2022).
467 doi:10.1101/2022.06.24.497495
- 468 6. Rodríguez-Beltrán, J., DelaFuente, J., León-Sampedro, R., MacLean, R. C. & San Millán, Á.
469 Beyond horizontal gene transfer: the role of plasmids in bacterial evolution. *Nat. Rev.*
470 *Microbiol.* 2021 **196** 347–359 (2021).
- 471 7. Millan, A. S., Escudero, J. A., Gifford, D. R., Mazel, D. & MacLean, R. C. Multicopy
472 plasmids potentiate the evolution of antibiotic resistance in bacteria. *Nat. Ecol. Evol.* 2016 **11** 1,
473 1–8 (2016).

474 8. Rodriguez-Beltran, J. *et al.* Multicopy plasmids allow bacteria to escape from fitness trade-offs
475 during evolutionary innovation. *Nat. Ecol. Evol.* 2018 **2**, 873–881 (2018).

476 9. Ilhan, J. *et al.* Segregational Drift and the Interplay between Plasmid Copy Number and
477 Evolvability. *Mol. Biol. Evol.* **36**, 472–486 (2019).

478 10. Garoña, A., Hülter, N. F., Romero Picazo, D. & Dagan, T. Segregational Drift Constrains the
479 Evolutionary Rate of Prokaryotic Plasmids. *Mol. Biol. Evol.* **38**, 5610–5624 (2021).

480 11. Birk, J. The Inheritance of Genes in Mitochondria and Chloroplasts: Laws, Mechanisms, and
481 Models. <http://dx.doi.org/10.1146/annurev.genet.35.102401.090231> **35**, 125–148 (2003).

482 12. Sonnenschein, E. C. *et al.* Global occurrence and heterogeneity of the Roseobacter-clade
483 species Ruegeria mobilis. *ISME J.* 2017 **11** **11**, 569–583 (2016).

484 13. Luo, H. & Moran, M. A. Evolutionary Ecology of the Marine Roseobacter Clade. *Microbiol.*
485 *Mol. Biol. Rev.* **78**, 573–587 (2014).

486 14. Gödeke, J., Paul, K., Lassak, J. & Thormann, K. M. Phage-induced lysis enhances biofilm
487 formation in *Shewanella oneidensis* MR-1. *ISME J.* 2011 **5**, 613–626 (2010).

488 15. Fan, H. & Chu, J. Y. A Brief Review of Short Tandem Repeat Mutation. *Genomics.*
489 *Proteomics Bioinformatics* **5**, 7–14 (2007).

490 16. Flynn, J. M., Lower, S. E., Barbash, D. A. & Clark, A. G. Rates and Patterns of Mutation in
491 Tandem Repetitive DNA in Six Independent Lineages of *Chlamydomonas reinhardtii*. *Genome*
492 *Biol. Evol.* **10**, 1673–1686 (2018).

493 17. Mitra, I. *et al.* Patterns of de novo tandem repeat mutations and their role in autism. *Nat.* 2020
494 **5897841** **589**, 246–250 (2021).

495 18. Lwoff, A. LYSOGENY. *Bacteriol. Rev.* **17**, 269–337 (1953).

496 19. Labrie, S. J., Samson, J. E. & Moineau, S. Bacteriophage resistance mechanisms. *Nat. Rev.*
497 *Microbiol.* 2010 **85** **8**, 317–327 (2010).

498 20. Yooseph, S. *et al.* Genomic and functional adaptation in surface ocean planktonic prokaryotes.
499 *Nature* **468**, 60–66 (2010).

500 21. Petersen, J. *et al.* A marine plasmid hitchhiking vast phylogenetic and geographic distances.
501 *Proc. Natl. Acad. Sci. U. S. A.* **116**, 20568–20573 (2019).

502 22. Yu, M. K., Fogarty, E. C. & Eren, A. M. The genetic and ecological landscape of plasmids in
503 the human gut. *bioRxiv* 2020.11.01.361691 (2022). doi:10.1101/2020.11.01.361691

504 23. Freese, H. M., Methner, A. & Overmann, J. Adaptation of Surface-Associated Bacteria to the
505 Open Ocean: A Genomically Distinct Subpopulation of *Phaeobacter gallaeciensis* Colonizes
506 Pacific Mesozooplankton. *Front. Microbiol.* **8**, 1659 (2017).

507 24. Freese, H. M. *et al.* Trajectories and Drivers of Genome Evolution in Surface-Associated
508 Marine *Phaeobacter*. *Genome Biol. Evol.* **9**, 3297–3311 (2017).

509 25. Wang, J. H. *et al.* Metagenomic analysis of antibiotic resistance genes in coastal industrial
510 mariculture systems. *Bioresour. Technol.* **253**, 235–243 (2018).

511 26. López-Pérez, M., Kimes, N. E., Haro-Moreno, J. M. & Rodriguez-Valera, F. Not all particles
512 are equal: The selective enrichment of particle-associated bacteria from the mediterranean sea.
513 *Front. Microbiol.* **7**, 996 (2016).

514 27. Nowinski, B. *et al.* Microbial metagenomes and metatranscriptomes during a coastal
515 phytoplankton bloom. *Sci. Data* 2019 **61** **6**, 1–7 (2019).

516 28. Moran, M. A. *et al.* Genome sequence of *Silicibacter pomeroyi* reveals adaptations to the

517 29. marine environment. *Nat. 2005 4327019* **432**, 910–913 (2004).

518 29. Fu, H., Uchimiya, M., Gore, J. & Moran, M. A. Ecological drivers of bacterial community
519 assembly in synthetic phycospheres. *Proc. Natl. Acad. Sci. U. S. A.* **117**, 3656–3662 (2020).

520 30. Jiang, H., Lei, R., Ding, S. W. & Zhu, S. Skewer: A fast and accurate adapter trimmer for next-
521 generation sequencing paired-end reads. *BMC Bioinformatics* **15**, 1–12 (2014).

522 31. Wick, R. R., Judd, L. M., Gorrie, C. L. & Holt, K. E. Unicycler: Resolving bacterial genome
523 assemblies from short and long sequencing reads. *PLOS Comput. Biol.* **13**, e1005595 (2017).

524 32. Wick, R. R., Schultz, M. B., Zobel, J. & Holt, K. E. Bandage: interactive visualization of de
525 novo genome assemblies. *Bioinformatics* **31**, 3350–3352 (2015).

526 33. Hyatt, D. *et al.* Prodigal: Prokaryotic gene recognition and translation initiation site
527 identification. *BMC Bioinformatics* **11**, 1–11 (2010).

528 34. Cantalapiedra, C. P., Herñandez-Plaza, A., Letunic, I., Bork, P. & Huerta-Cepas, J. eggNOG-
529 mapper v2: Functional Annotation, Orthology Assignments, and Domain Prediction at the
530 Metagenomic Scale. *Mol. Biol. Evol.* **38**, 5825–5829 (2021).

531 35. Li, H. Minimap2: pairwise alignment for nucleotide sequences. *Bioinformatics* **34**, 3094–3100
532 (2018).

533 36. Li, H. *et al.* The Sequence Alignment/Map format and SAMtools. *Bioinformatics* **25**, 2078–
534 2079 (2009).

535 37. Schwartzman, J. A. *et al.* Bacterial growth in multicellular aggregates leads to the emergence
536 of complex lifecycles. *bioRxiv* 2021.11.01.466752 (2021). doi:10.1101/2021.11.01.466752

537 38. Langmead, B. & Salzberg, S. L. Fast gapped-read alignment with Bowtie 2. *Nat. Methods* **2012**
538 **9**, 357–359 (2012).

539 39. Anders, S., Pyl, P. T. & Huber, W. HTSeq—a Python framework to work with high-throughput
540 sequencing data. *Bioinformatics* **31**, 166–169 (2015).

541 40. Love, M. I., Huber, W. & Anders, S. Moderated estimation of fold change and dispersion for
542 RNA-seq data with DESeq2. *Genome Biol.* **15**, 1–21 (2014).

543 41. Schneider, C. A., Rasband, W. S. & Eliceiri, K. W. NIH Image to ImageJ: 25 years of image
544 analysis. *Nat. Methods* **2012** **9**, 671–675 (2012).

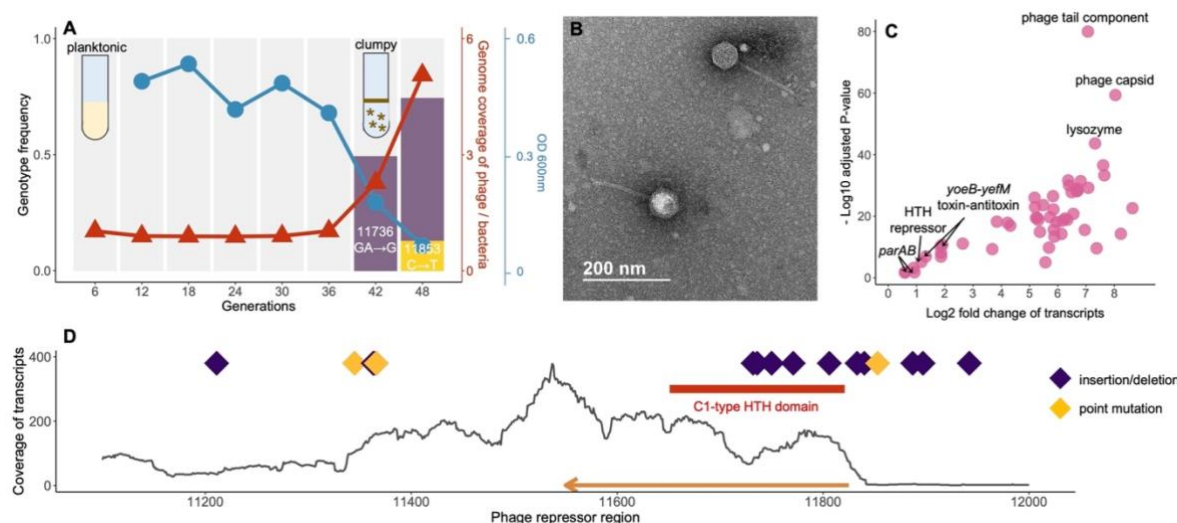
545 42. Kieft, K., Zhou, Z. & Anantharaman, K. VIBRANT: Automated recovery, annotation and
546 curation of microbial viruses, and evaluation of viral community function from genomic
547 sequences. *Microbiome* **8**, 1–23 (2020).

548 43. Steinegger, M. & Söding, J. MMseqs2 enables sensitive protein sequence searching for the
549 analysis of massive data sets. *Nat. Biotechnol.* **2017 3511** **35**, 1026–1028 (2017).

550 44. Parada, V., Herndl, G. J. & Weinbauer, M. G. Viral burst size of heterotrophic prokaryotes in
551 aquatic systems. *J. Mar. Biol. Assoc. United Kingdom* **86**, 613–621 (2006).

552 45. Weitz, J. S., Li, G., Gulbudak, H., Cortez, M. H. & Whitaker, R. J. Viral invasion fitness across
553 a continuum from lysis to latency. *Virus Evol.* **5**, (2019).

554
555
556
557
558



559

560 **Figure 1 Mutations in a phage repressor region recurrently drives productive infection of the**
561 **phage-plasmid. (A)** Productive switch of a phage-plasmid in *Tritonibacter mobilis* A3R06 was
562 observed after ~40 generations of serial-dilution growth (red). A deletion mutation (11736: GA→G,
563 purple bar) rapidly increased to ~50% relative genotypic frequency within one dilution cycle, before
564 the increase slowed down in the next dilution cycle. A second mutation (11853: C→T, yellow bar)
565 was observed in the last dilution cycle. Planktonic bacterial culture became highly clumpy after the
566 productive switch, as indicated by the sharp decrease in OD600 (blue). For eco-evolutionary
567 trajectories for the other 8 populations temporally-tracked with genomic sequencing, see Figure S4
568 and Table S1. **(B)** Transmission electron microscope image of the phage-plasmid particle. **(C)**
569 Differential expression of phage-plasmid genes before and after observing the mutation. Genes
570 related to phage production were significantly upregulated after the productive switch, in particular
571 the phage structural genes and the phage lysozyme gene. Expression of genes that are housekeeping
572 for plasmid replication and stability were only increased because of copy-number increase of genes.
573 **(D)** All 21 mutations identified in 15 independent lines of populations were within a short ~1,000
574 bp region encoding a C1-type phage repressor (orange arrow). Most of mutations are insertions or
575 deletions (purple diamond). Details of these mutations are listed in Table S1.

576

577

578

579

580

581

582

583

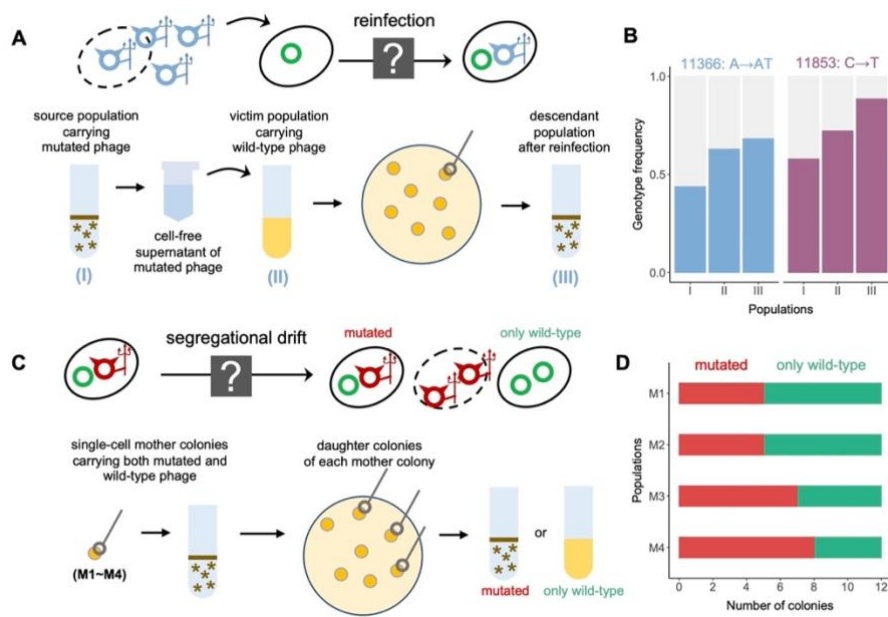
584

585

586

587

588



589

590 **Figure 2 Experimental confirmation of reinfection and segregational drift.** (A) Schematic
591 illustration of reinfection, for which we hypothesize that mutated phages are able to infect hosts
592 lysogenized by wild-type phages. Wild-type and mutated phage-plasmids were showed as green
593 circles and blue color circles. See Methods for full experimental details. (B) Mutated phages with
594 the same genotype were observed across (I) the initial source host population carrying the mutated
595 phage, (II) the victim host population re-infected by the mutated phage and (III) the descendant of
596 (II), supporting our hypothesis of reinfection. Experiments were performed in biological duplicates
597 with two source host populations carrying different genotypes of mutated phages (blue and purple).
598 (C) Schematic illustration of segregational drift, for which we hypothesize that a host infected by
599 mutated phages is able to generate offspring with only wild-type phages. See Methods for full
600 experimental details. (D) Each of the 4 single-cell mother colonies (M1~M4) carrying a mixture of
601 mutated phages and wild-type phages was able to generate descendants only carrying the wild-type
602 phages, supporting our hypothesis of segregational drift.

603

604

605

606

607

608

609

610

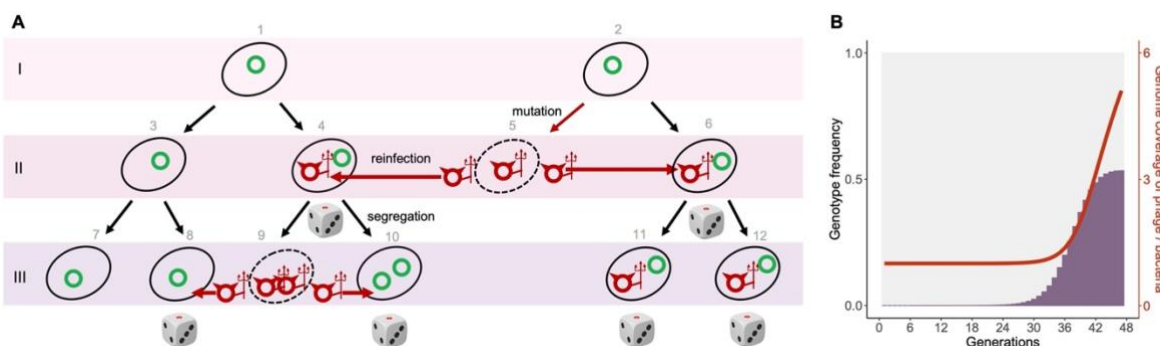
611

612

613

614

615



616

617 **Figure 3 A minimal model for phage-plasmid hybrid reproduces the observed eco-
618 evolutionary dynamics. (A)** Schematic illustration of the model simulation. A dice is drawn under
619 a host cell when it carries more than one copies of phage-plasmids with different genotypes (a
620 heterozygote). In those cases, the phage-plasmid genotype in descendants becomes stochastic due
621 to segregational drift (e.g., cells 9, 10, 11 and 12). **(B)** With reinfection and segregational drift as the
622 only two components, the simulated eco-evolutionary dynamics well matches the observed patterns
623 in the experiment. For the experimentally observed eco-evolutionary dynamics, see Fig. 1a and Fig.
624 S4. See Methods for full details of the model simulation.

625

626

627

628

629

630

631

632

633

634

635

636

637

638

639

640

641

642

643

644

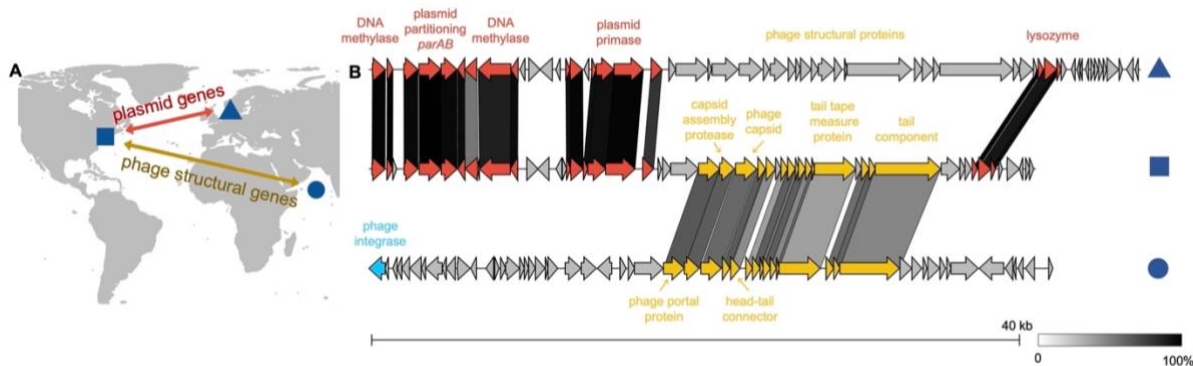
645

646

647

648

649



650

651 **Figure 4 The same plasmid backbone carrying different phage genes disseminate vast**
652 **geographic distance.** *Tritonibacter mobilis* M41-2.2, isolated in Denmark, contains a phage-
653 plasmid (triangle) whose plasmid-related genes are homologous and syntetic to those of
654 *Tritonibacter mobilis* A3R06 phage-plasmid (square). However, their phage structural genes are
655 very different from each other. Phage structural genes of *Tritonibacter mobilis* A3R06 phage-
656 plasmid is both homologous and syntetic to that of a chromosome-integrated phage found in
657 *Roseobacter* sp. SK209-2-6 (circle), which was isolated from deep water column in the Arabian Sea.

658

659

660

661

662

663

664

665

666

667

668

669

670

671

672

673

674

675

676

677

678